Ecological Modelling 226 (2012) 22–35

Contents lists available at SciVerse ScienceDirect

Ecological Modelling

journal homepage: www.elsevier.com/locate/ecolmodel

Estimation of crown biomass of *Pinus pinaster* stands and shrubland above-ground biomass using forest inventory data, remotely sensed imagery and spatial prediction models

H. Viana[a,b,*], J. Aranha[b], D. Lopes[b], Warren B. Cohen[c]

[a] *Centro de Estudos em Educação, Tecnologias e Saúde, Agrarian Superior School, Polytechnic Institute of Viseu, Quinta da Alagoa, 3500-606 Viseu, Portugal*
[b] *CITAB, University of Trás-os-Montes e Alto Douro, Apartado 1014, 5001-801 Vila Real, Portugal*
[c] *USDA Forest Service, 3200 SW Jefferson Way, Corvallis, OR 97331, USA*

ARTICLE INFO

Article history:
Received 28 March 2011
Received in revised form
16 November 2011
Accepted 25 November 2011

Keywords:
Above-ground biomass
Remote sensing
Geostatistics
Regression-kriging
Pinus pinaster
Shrubland

ABSTRACT

Spatially crown biomass of *Pinus pinaster* stands and shrubland above-ground biomass (AGB) estimation was carried-out in a region located in Centre-North Portugal, by means of different approaches including forest inventory data, remotely sensed imagery and spatial prediction models. Two cover types (pine stands and shrubland) were inventoried and biomass assessed in a total of 276 sample field plots. We compared AGB spatial predictions derived from Direct Radiometric Relationships (DRR) of remotely sensed data; and the geostatistical method Regression-kriging (RK), using remotely sensed data as auxiliary variables. Also, Ordinary Kriging (OK), Universal Kriging (UK), Inverse Distance Weighted (IDW) and Thiessen Polygons estimations were performed and tested. The comparison of AGB maps shows distinct predictions among DRR and RK; and Kriging and deterministic methods, indicating the inadequacy from these later ones to map AGB over large areas. DRR and RK methods produced lower statistical error values, in pine stands and shrubland, when compared to kriging and deterministic interpolators. Since forest landscape is not continuous variable, the tested forest variables showed low spatial autocorrelation, which makes kriging methods unsuitable to these purposes. Despite the geostatistical method RK did not increase the accuracy of estimates developed by DRR, denser sampling schemes and different auxiliary variables should be explored, in order to test if the accuracy of predictions is improved.

1. Introduction

1.1. Biomass spatial prediction

Estimates of above-ground biomass (AGB) of forested areas have been used to address a broad range of questions including estimations of forest productivity (Chirici et al., 2007; Palmer et al., 2009), studying the impacts of forest fires or other disturbances (García-Martín et al., 2008), monitoring the biomass changes over time (Hu and Wang, 2008), assessing the forest biomass for use as energy (Viana et al., 2010) or to estimate the global carbon balance (Hese et al., 2005). Nowadays, the analysis of these issues over large areas is a common practice. The need of continuous maps where the phenomenon under study can be individually analysed or used as auxiliary variable in a specific model requires that the spatial predictions are represented in the most accurate way. Estimation of AGB has been made by a range of methods, from field measurements to remote sensing-based methods, as well GIS-based modelling approaches using auxiliary data (Lu, 2006).

Traditional approaches to estimate forest AGB over a large area consist in the implementation of forest inventories where a statistical sampling design is established to acquire data, or using data aggregated from stand level management inventories (McRoberts et al., 2010). Estimation using sample-based inventories involves field measurements where AGB is commonly assessed by applying allometric equations for specific species (Ter-Mikaelian and Korzukhin, 1997; Foroughbakhch et al., 2005; Zianis et al., 2005; Peichl and Arain, 2007), at the tree or shrub level, using the dendrometric variables (e.g. diameter-at-breast height, tree height, crown size and crown length) measured in each sample plot. The total biomass for a given area is achieved by applying expansion factors to the area of the sample plot and stand conversion tables. These approaches are widely used in several studies (e.g. Brown et al., 1989; Brown and Lugo, 1992; Fearnside, 1992; Gillespie et al., 1992; Fearnside, 1997; Houghton et al., 2001; Fournier et al., 2003). These estimation models are considered non-spatial as they do not provide the spatial distribution of AGB. To predict the spatial distribution of AGB throughout the territory, the calculated AGB in the

* Corresponding author at: Agrarian Superior School, Polytechnic Institute of Viseu, Quinta da Alagoa, 3500-606 Viseu, Portugal. Tel.: +351 232 446 600; fax: +351 232 426 536.
E-mail addresses: hviana@esav.ipv.pt, viana.h@gmail.com (H. Viana).

0304-3800/$ – see front matter © 2011 Elsevier B.V. All rights reserved.
doi:10.1016/j.ecolmodel.2011.11.027

forest inventory dataset is usually assigned to the forest polygons, stratified by species, and mapped by aerial photo interpretation.

Despite the field measurements being the most accurate methods for collecting biomass data, the level of precision of the resultant biomass map will depend of the land cover classification detail and of the sample intensity. In fact, the forest inventories data at regional or national scale are usually not spatially exhaustive to generate spatially AGB estimates, thus limiting the use of this approach over large areas. An additional limitation is the long temporal resolution of these estimations, which are made in cycles of 10 or more years. This is not compatible with the need of information on shorter time intervals, to analyse land cover changes, to quantify forest resources, or to monitor other environmental variables. In order to overcome these limitations and the need to produce more accurate spatially explicit large area biomass estimates led the researchers to explore different approaches to mapping biomass.

With the increasing availability of satellite imagery, remote sensing-based methods have been the most widely used approach to predict AGB over large areas, in recent years. The utility of the spectral information recorded by remote sensing for monitoring vegetation or gathering ecophysiological information over large areas is very well recognized (Jong et al., 2006), since satellite data became accessible for land cover dynamic studies. It has been demonstrated in several studies that the satellite spectral information (spectral band, band ratios, band transformations, etc.) has a good correlation with forest biomass and when combined with field measurements, is suitable for AGB estimation. Previous research using imagery data provided by distinct sensors and employing different approaches are summarized by Lu (2006). Although remotely sensed data cannot completely replace field sample data, it have been incorporated into operational forest inventories (McRoberts et al., 2010).

Several studies using remotely sensed data sources with different spatial-resolution and applying distinct approaches have been conducted in AGB spatial predictions. These approaches include direct estimations by means of Direct Radiometric Relationships (DRR), between spectral data response and biomass amount, using multiple regression analysis (Hame et al., 1997; Cohen et al., 2001, 2003; Reich et al., 2004; Labrecque et al., 2006; Muukkonen and Heiskanen, 2007; Zheng et al., 2007); by nonparametric approaches including K nearest neighbour (KNN) (Tomppo, 1991; Reese et al., 2002; Tomppo et al., 2002; Labrecque et al., 2006; Chirici et al., 2008; Tomppo et al., 2008) and neural network (Atkinson and Tatnall, 1997; Blackard and Dean, 1999; Muukkonen and Heiskanen, 2005), or indirect estimations. Is this case, characteristics such as crown diameter or leaf area index (LAI) are firstly derived from the remotely sensed data and subsequently are used in regression analysis to estimate biomass.

GIS-based approaches (Iverson et al., 1994; Magcale-Macandog et al., 2006) using ancillary data (e.g. Elevation, slope, soil, precipitation, etc.) have not been applied extensively for AGB estimation given the low availability of data, often not sufficiently precise, and the frequent low correlation between AGB and ancillary data.

Spatial models (algorithms) have been also used for spatially predict vegetation attributes. In general, these interpolation techniques are classified in deterministic and probabilistic models (Isaaks and Srivastava, 1989; Goovaerts, 1997; Burrough and McDonnell, 1998; Hengl, 2009). The deterministic approaches are models where arbitrary or empirical model parameters are used. No estimate of the model error is available and usually no strict assumptions about the variability of a feature exist (Hengl, 2009). Inverse distance weighting (IDW) and Thiessen polygons are the most widely used approach to execute interpolations and, in some situations, these can perform as well, or better, than other spatial prediction methods (Weber and Englund, 1992; Hengl, 2009). Attending that in the Earth sciences there is usually a lack of sufficient knowledge concerning how properties vary in space, a deterministic model may not be appropriate. Therefore, to make predictions at locations for which observations do not exist, with inherent uncertainty in predictions, the use of probabilistic models are necessary (Lloyd, 2007).

Spatial statistics and geostatistics were developed to describe and analyse the variation in both natural and man-made phenomena on, above or below the land surface (Cressie, 1993). Geostatistical models are reported in numerous textbooks (e.g. Isaaks and Srivastava, 1989; Cressie, 1993; Goovaerts, 1997; Deutsch and Journel, 1998; Hengl, 2009) such as Kriging (plain geostatistics); environmental correlation (e.g. regression-based); Bayesian-based models (e.g. Bayesian Maximum Entropy) and hybrid models (e.g. regression-kriging). Largely developed by Matheron (1963) in the 1960s, to evaluate recoverable reserves for the mining industry, over the years geostatistical models have been applied in a wide range of fields including modelling forest structure and attributes. Geostatistics and the theory of regionalized variables (Matheron, 1971) has been used to (Curran and Atkinson, 1988): explore and describe the presence of spatial variation that occur in most natural resource variables and in remotely sensed data (Curran, 1988; Woodcock et al., 1988); to design optimum sampling schemes for image data and ground data (McBratney and Webster, 1981; Hernández and Emery, 2009); and to increase the accuracy in which remotely sensed data can be used to classify land cover (Zhang and Franklin, 2002; Buddenbaum et al., 2005).

In recent years, several works has been conducted using geostatistical approaches to predict continuous forest variables. The motivation for using geostatistical analysis is that classical design-based methods are often weak for small area estimation within global inventories, and there is also an increasing demand to use regional or national inventory data for local estimation purposes (Mandallaz, 1993). However, the major limitation in using spatial statistical models is when forest variable datasets are spatially independent the lack of spatial structure makes it difficult, if not impossible to use optimal predictors such as Ordinary Kriging for modelling the spatial variability in the data (Reich et al., 2011). In a particular stand level spatial distribution of tree attributes i.e., basal area, height and density can be thought to be directly influenced by different spatially continuous variables such as solar radiation, soil characteristics and water nutrient availability, thus allowing considered spatially continuous (Kint et al., 2003).

Geostatistics has been used for mapping forest variables (e.g. basal area, density, LAI, tree height, standing volume, above-ground biomass, productivity, etc.) based on forest inventory data where these variables seemingly have spatial autocorrelation (Dungan, 1998; Nanos et al., 2004; Berterretche et al., 2005; Maselli and Chiesi, 2006; Mutanga and Rugege, 2006; Sales et al., 2007; Meng et al., 2009; Palmer et al., 2009; Pierce et al., 2009; Akhavan and Kia-Daliri, 2010). However, in large areas forest variables as AGB is not always spatially continuous because it is highly dependent on forest landscape structure and boundaries of forest patches affected by clear-cuttings of commercial forest management. Gilbert and Lowell (1997) trying to predict stem volume measured the spatial autocorrelation of two interpolation methods Thiessen polygons and kriging concluded that although areas of high volume do tend to cluster, i.e. are positively spatially autocorrelated, the forest did not behave as a continuous surface relative even to the densest sampling schema. Gunnarsson et al. (1998) used kriging estimation of stand variables such as total volume, annual volume increment, mean diameter and age and found positive autocorrelation. However, some variables (e.g. hardwood volume) does not exhibited any spatial autocorrelation in the scales studied, suggesting that only conducting an a priori assessment of spatial autocorrelation to determine interpolability may be misleading. Tuominen et al. (2003) combining data from remote sensing imagery with field measurements, and geostatistical interpolation for estimation of five forest variables (mean diameter, mean height, mean age, basal area, and volume) per sample plot and stand, found that the geostatistical interpolation, tested on the stand level estimation, did not improve the accuracy of the estimates. The same conclusion was reported by Freeman and Moisen (2007) who evaluating Kriging as a tool to improve forest biomass estimates concluded that map accuracy was not increased.

While some geostatistical models, such as Kriging, may not provide the desired solution to map AGB over large areas, it is necessary to explore new approaches. The studies exploring spatial prediction models Regression-kriging (RK) using field observations, in combination with various GIS data sources (e.g. remotely sensed data, soil and topographic variables, forest structure, etc.), as auxiliary information are not plentiful. However, some studies indicated good improvements using these approaches on forest variable estimation as volume mean annual increment (Palmer et al., 2009); basal area (Meng et al., 2009) and above-ground biomass (Sales et al., 2007), in comparison with other prediction methods.

In this study, we analysed different approaches to estimate crown biomass of *Pinus pinaster* stands and above-ground biomass of shrubland, including: direct radiometric relationships (DRR) methods and Regression-kriging (RK) with remotely sensed data as predictor. Moreover, deterministic interpolation techniques as Inverse distance weighting (IDW) and Thiessen polygons, and Kriging estimations are presented in order to compare the performance of these methods in large-scale mapping of forest biomass.

1.2. Direct Radiometric Relationships (DRR)

This method consist in establishing regression relationships, such as ordinary least squares (OLS), between the satellite spectral data, which can include the individual spectral bands, band ratios, vegetation indices and other possible transformations as independent variables, and the measured biomass at each corresponding inventory sample plot position. In this work, Landsat 5 TM and MODIS Vegetation indices were used as independent variables since they are referred in the literature as being well correlated with biomass availability.

1.3. Inverse Distance Weighting (IDW)

Inverse distance weighting (IDW) is a quick deterministic local interpolator that is exact and can be a good method to perform a preliminary analysis of an interpolated surface. It is often used as the default surface generation method to attribute sample locations (Lu and Wong, 2008). IDW explicitly implements the assumption that a value of an attribute at an unsampled location is a weighted average of known data points within a local neighbourhood surrounding the unsampled location (Burrough and McDonnell, 1998). To predict a value for any unsampled location, IDW will use the measured values surrounding the prediction location. Those measured values closest to the prediction location will have more influence on the predicted value than those farther away. Thus, the IDW formula has the effect of giving data points close to the interpolation point relatively large weights while those far away exert little influence. The higher the weight used the more influence points close to prediction location are given. The IDW predictor can be given as (Eq. (1)):

$$\hat{z}(x_0) = \frac{\sum_{i=1}^{n} z(x_i).d_{i0}^{-r}}{\sum_{i=1}^{n} d_{i0}^{-r}} \tag{1}$$

where the prediction for the location x_0 is a function of the n neighbouring observations, $z(x_i)$, $i = 1; 2; \ldots; n$, r is an exponent which determines the weight assigned to each of the observations, and d is the distance by which the prediction location x_0 and the observation location x_i are separated.

As the exponent becomes larger the weight assigned to observations at large distance from the prediction location becomes smaller. That is, as the exponent is increased, the predictions become more similar to the closest observations.

1.4. Thiessen polygons: nearest neighbours

Thiessen polygons also called Dirichlet or Voronoi polygons assign values to unsampled locations that are equal to the value of the nearest observation (Lloyd, 2007). This method is one of the earliest and simplest interpolation methods. They have been considered one of the fundamental structures in computational geometry and other fields such as GIS. In this method, the study area is partitioned into a set of polygons, each containing only one measurement point. Every point within a given polygon is closer to the measurement point than any other measurement points.

The region sampled, R, is divided by perpendicular bisectors between the N sampling points into polygons or tiles, V_i, $i = 1, 2, \ldots, N$, such that in each polygon all points are nearer to its enclosed sampling point x_i than to any other sampling point. The prediction at each point in V_i is the measured value at x_i, i.e. $z^*(x_0) = Z(x_i)$. The weights are (Webster and Oliver, 2007):

$$\lambda_i = \begin{cases} 1 & fx_i \in V_i \\ 0 & \text{otherwise} \end{cases}$$

The shortcomings of the method are evident; each prediction is based on just one measurement, there is no estimate of the error, and information from neighbouring points is ignored. When used for mapping the result is basic (Webster and Oliver, 2007). However, Thiessen polygons are used widely to provide a simple overview of the spatial distribution of values.

1.5. Ordinary Kriging (OK)

Kriging originated by (Krige, 1951) and developed by (Matheron, 1971) is widely known by the acronym BLUP, because it is the best linear unbiased predictor. The theory and mathematical formulation of kriging have been discussed thoroughly by several authors (e.g. Journel and Huijbregts, 1978; Isaaks and Srivastava, 1989; Cressie, 1993; Goovaerts, 1997). Kriging is a geostatistical method that takes into account both the distance and the degree of variation between known data points. The extent to which this assumption is true can be examined in the computed variogram. The several kriging models (kriging family) are elaborations of the basic generalized linear regression algorithm and corresponding estimator (Eq. (2)) differing by some assumptions (or knowledge) on the data (process) (Goovaerts, 1997; Deutsch and Journel, 1998):

$$[\hat{Z}_k(u) - m(u)] = \sum_{\alpha=1}^{n} \lambda_\alpha(u)[Z(u_\alpha) - m(u_\alpha)] \tag{2}$$

where $Z(u)$ is the random variable at location u, the u_α is the n data locations, $\lambda_\alpha(u)$ is the weight assigned to datum $Z(u_\alpha)$ which is a realization of $Z(u_\alpha)$, $m(u)$ and $m(u_\alpha)$ are the location-dependent expected value of $Z(u)$ and $Z(u_\alpha)$, and $\hat{Z}_k(u)$ is the linear regression estimator.

Ordinary Kriging (OK) filters the mean from Eq. (2) by requiring that the Kriging weights sum to one. The OK prediction $\hat{Z}_{OK}(u)$ is a linear weighted moving average of the available n observations defined as (Deutsch and Journel, 1998) (Eq. (3)):

$$\hat{Z}_{OK}(u) = \sum_{\alpha=1}^{n} \lambda_\alpha^{OK}(u) Z(u_\alpha) \tag{3}$$

Using Lagrange form, OK system is written as:

$$\begin{cases} \sum_{\beta=1}^{n} \lambda_{\beta}^{\mathrm{OK}}(u) C(u_{\beta} - u_{\alpha}) + \mu_{\mathrm{OK}}(u) = C(u - u_{\alpha}) \\ \sum_{\beta=1}^{n} \lambda_{\beta}^{\mathrm{OK}}(u) = 1 \end{cases} \quad (\alpha = 1, \ldots, n)$$

where $\lambda_{\beta}^{\mathrm{OK}}(u)$ is the optimal weight, $C(u-u_{\alpha})$ is the covariance function between two points, and $\mu_{\mathrm{OK}}(u)$ is the Lagrange parameter.

The corresponding minimized error variance, also called OK variance is expressed as (Eq. (4)):

$$\sigma_{\mathrm{OK}}^2 = C(0) - \sum_{\alpha=1}^{n} \lambda_{\alpha}^{\mathrm{OK}} C(u_{\alpha} - u) - \mu_{\mathrm{OK}}(u) \quad (4)$$

The Ordinary Kriging cannot be used unless the regionalized variable has a constant mean although it is not known. Because the successive differences conceal the regional mean in the semivariogram calculations, this means that in the case of a systematic variation in the regional average such as abrupt changes, trends, oscillations, the Ordinary Kriging assumption of constant mean is violated. Therefore other estimation procedure, which should take into consideration these systematic mean variations, must be used (Sen, 2009).

1.6. Universal Kriging (UK) or kriging with internal drift

"Universal kriging" (UK), first introduced by Matheron (1969), is as a special case of kriging with changing mean where the trend is modelled as a function of cartographic coordinates (Deutsch and Journel, 1998; Webster and Oliver, 2007). Deutsch and Journel (1998) define this method as kriging with a trend model since the underlying random function model $Z(u)$ is the sum of a trend component, $m(u)$ plus a residual $R(u)$ (Eq. (5)):

$$Z(u) = m(u) + R(u) \quad (5)$$

The trend m is a deterministic, structural component that represents large scale variation. The residual is a stochastic component representing small scale, 'noisy' variation. The trend component is defined as $m(u)=E\{Z(u)\}$, and is fitted as $m(u) = \sum_{k=0}^{K} a_k f_k(u)$. The $f_k(u)$'s are known functions of the location coordinates and the a_k's are unknown parameters. The trend value $m(u)$ is itself unknown since the parameters a_k are unknown. The residual component $R(u)$ is usually modelled as a stationary random function with zero mean and covariance $C_R(h)$.

Using Lagrange formalism, UK system is written as:

$$\begin{cases} \sum_{\beta=1}^{n} \lambda_{\beta}^{\mathrm{UK}}(u) C_R(u_{\alpha} - u_{\beta}) + \sum_{k=0}^{K} u_k^{\mathrm{UK}}(u) f_k(u_{\alpha}) = C_R(u_{\alpha} - u) \\ \sum_{\beta=1}^{n} \lambda_{\beta}^{\mathrm{UK}}(u) = 1, \quad \sum_{\beta=1}^{n} \lambda_{\beta}^{\mathrm{UK}}(u) f_k(u_{\beta}) = f_k(u) \end{cases} \quad (\alpha = 1, \ldots, n), (k = 0, \ldots, k)$$

where $\lambda_{\beta}^{\mathrm{UK}}(u)$ is the optimal weight, $C_R(u_{\alpha}-u_{\beta})$ is the covariance function between two residual points, and $u_k^{\mathrm{UK}}(u)$ is the Lagrange parameter.

The corresponding UK variance σ_{UK}^2 is (Eq. (6)):

$$\sigma_{\mathrm{UK}}^2(u) = C_R(0) - \sum_{\alpha=1}^{n} \lambda_{\alpha}^{\mathrm{UK}} C_R(u_{\alpha} - u) - \sum_{k=0}^{k} u_k^{\mathrm{UK}}(u) f_K(u) \quad (6)$$

1.7. Regression-kriging (RK)

Regression-kriging (RK) (Odeh et al., 1994, 1995) is a hybrid method that involves either a simple or multiple-linear regression model (or a variant of the generalized linear model and regression trees) between the target variable and ancillary variables, calculating residuals of the regression, and combining them with kriging. Different types or variant of this process, but with similar procedures, can be found in literature, which can cause confusion in the computational process. RK defined by Ahmed and De Marsily (1987) as "Kriging with a guess field" involves regression, and calculation of the residuals. This is followed by kriging of the regression predicted values and the residuals separately, and summing both values together to obtain the final prediction. Knotters et al. (1995) define this method as "kriging combined with regression" where regression is performed, and followed by kriging of regressed values, whereas Goovaerts (1999) uses the term "Kriging after detrending" to refer the RK method. Hengl et al. (2004, 2007) makes a comprehensive analysis to the RK spatial prediction technique and compared it with the Kriging with external drift (KED) method (Goovaerts, 1997) concluding that they are equivalent and should, under the same assumptions, yield the same predictions.

In this paper we refer to RK according to Hengl et al. (2007) and Hengl (2009) and the proposed methodology of implementation (http://spatial-analyst.net) is followed. In the process of RK the predictions are combined from two parts; one is the estimate $\hat{m}(s_0)$ obtained by regressing the primary variable on the k auxiliary variables $q_k(s_0)$ and $q_0(s_0)=1$; the second part is the residual estimated from kriging. RK is estimated as follows (Eqs. (7) and (8)):

$$\hat{z}_{rk}(s_0) = \hat{m}(s_0) + \hat{e}(s_0) \quad (7)$$

$$\hat{z}_{rk}(s_0) = \sum_{k=0}^{v} \hat{\beta}_k \cdot q_k(s_0) + \sum_{i=1}^{n} w_i(s_0) \cdot e(s_i) \quad (8)$$

where $\hat{\beta}_k$ are estimated drift model coefficients ($\hat{\beta}_0$ is the estimated intercept), optimally estimated from the sample by some fitting method, e.g. ordinary least squares (OLS) or, optimally, using generalized least squares (GLS), to take the spatial correlation between individual observations into account (Cressie, 1993); w_i are kriging weights determined by the spatial dependence structure of the residual and $e(s_i)$ are the regression residuals at location s_i.

2. Methods and data

2.1. Study area

The study area is located in the Centre-North of Portugal, extending from 39°11′53″N, 06°14′17″W to 42°50′50″N, 08°19′02″W (Fig. 1a). This is a heterogeneous region with a complex topography where the elevations ranging from 130 to 1500 m (Fig. 1b). The climatic factors are very variable during the year, with annual mean precipitation in the range of 800–2800 mm and annual mean temperatures ranging from 7.5 to 16 °C. These physical conditions make this region well-suited for forest growth. The land cover is fragmented with small amount of suitable soils for agriculture and the main areas are occupied by forest spaces. Forest activity is a direct source of income for a vast forest products industry, which employs a significant part of the population.

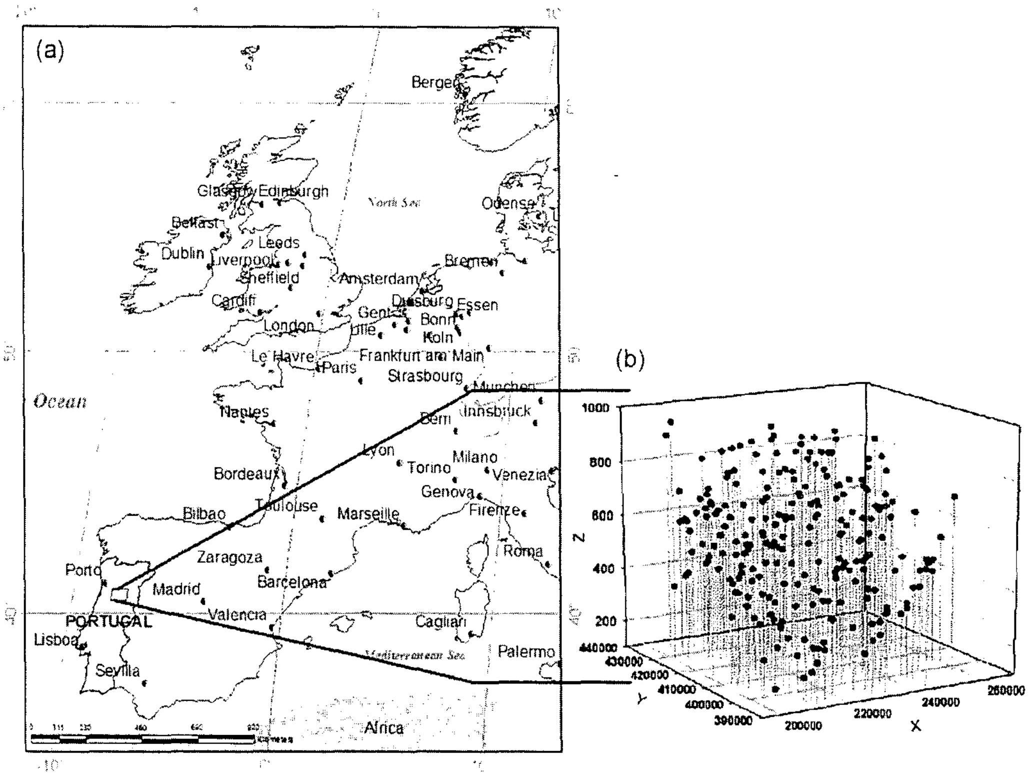

Fig. 1. Study area: (a) Geographical location, (b) Distribution of inventory samples plots, where x, y are the cartographic coordinates (Hayford-Gauss, Datum of Lisbon, IGeoE) and z is the altitude (m).

2.2. Field data

A systematic sampling design was implemented in the study area which include productive forest stands and shrubland areas. A total of 276 sample plots were located being 102 from shrubs, 132 from pure *P. pinaster* Aiton (maritime pine) stands and the remaining plots from *Eucalyptus globulus* (eucalyptus) and mixed stands. For the purpose of the present study, only the pure pine stands and shrubland areas were considered. The field data was collected in circular temporary sample plots within a fixed-area of 500 m^2, in the year 2006. The plots geographical locations were recorded by global navigation satellite systems (GNSS), georeferenced and structured in a geographic information system (GIS) database. In pine stands, the dendrometric parameters: diameter at breast height (dbh), total height of the tree (h) and canopy height (hc) were measured. The structural stand variables recorded in each plot were used to determine the stand characteristics such as age (t), number of trees per hectare (N), dominant tree height class (h_{dom}), basal area (G), crown closure class and site index (SI). In the shrubland areas the dominant height of vegetation (h_{dom}), the vegetation cover (%) and species composition were determined. This data was recorded in a GIS geodatabase, in the Portuguese Cartographic coordinates, to further analysis.

2.3. Biomass calculation from the inventory dataset

In order to achieve the biomass in the inventory dataset, different methodologies were followed for the two cover classes considered in the present study. In the pine stands only the so-called primary residues (parts of trees, unsuitable for saw timber such as branches and tops) were calculated and used in the spatially explicit biomass estimation (crown biomass), while for the shrub biomass the entire above-ground biomass was used. This option was due to the fact that the primary residues from pine stands and the shrubland biomass are often ignored in biomass estimations, and their use for energy has being increasing in the last years. As example, the Portuguese political strategy to generate combined heat and power (CHP) from biomass states that the main source of fuel should come from the residual biomass generated by forest activity, where the crown biomass represents the majority, and the other source of fuel should come from shrubs with the intention of reducing the wildfire hazard (see Viana et al., 2010). On the other hand, the isolated canopy cover had better adjustments with the spectral information extracted from the Landsat TM imagery data, than the biomass of the entire tree (stem and crown). In fact, after the canopy cover reaches its maximum the stem keep growing but the changes in reflectance are very small.

The crown biomass of pine stands was calculated using an allometric equation adjusted for the study area, which are presented further in Section 3.2, Table 2. A total of 100 trees were sampled within 10 maritime pine stands, using the destructive method. The trees were logged, measured (e.g. diameter at breast height, total height, canopy height) and the live crown weighted in situ. The moist content was determined in laboratory, for the conversion of biomass to dry weight. The measured variables were then used for adjustment of regression models, using the crown biomass (kg tree^{-1}) as dependent variable. To estimate the shrubland biomass 20 sample plots, with an area of 10 m^2, were established and the vegetation parameters measured (shrubs density, height and estimated age) using the line intersection method. The vegetation was divided by species composition and the total biomass was weighted in loco. The measured variables were used for adjustment of regression models using shrub AGB (ton ha^{-1}) as dependent variable, which are presented further in Section 3.2,

Table 1
Descriptive statistics of data measured in the inventory dataset.

	Pine stands plots (n = 132)								Shrubland plots (n = 102)	
	N (trees ha^{-1})	t (year)	h_{dom} (m)	dbh$_{dom}$ (cm)	SI (m)	BA (m^2 ha^{-1})	V (m^3 ha^{-1})	B_{cb} (ton ha^{-1})	Canopy cover (%)	B_{sr} (ton ha^{-1})
Mean	550.8	24.4	15.3	29.7	25.7	20.1	164.6	17.7	56.1	12.0
Min	20.0	8.0	6.0	10.8	16.5	0.4	1.4	1.3	5.0	0.795
Max	2138.5	51.0	29.4	69.9	40.1	68.3	574.1	39.9	100.0	36
SD	372.0	12.0	5.7	10.7	4.6	13.1	129.3	10.1	25.33	8.12

Where N is the number of stems; t is the stand age; h_{dom} is the dominant height; dbh$_{dom}$ is the dominant diameter at breast height; SI is the site index and is presented as meters at 35 years old; BA is the basal area; V is the stand commercial volume; B_{cb} is the biomass of crown and B_{sr} is the weight on dry base of biomass measured in the shrubland sample plots and n is the number of sampling plots established.

Table 2. These equations were then applied to calculate the AGB in the inventory dataset, according to the stand and shrub characteristics of each sample plot.

2.4. Remote sensing procedures

2.4.1. Remote sensing data

Two different remote sensing imagery data freely available from the US Geological Survey (USGS) Earth Resources Observation and Science (EROS) Centre were used in this research. A Landsat 5 Thematic Mapper (TM) image (Path/row: 204/032) acquired on 10 December 2006 and the Global MODIS vegetation indices dataset (h17v04) from the Moderate Resolution Imaging Spectroradiometer (MODIS) from 29 August 2006 (MOD13Q1.A2006241.h17v04.005.2008105184154.hdf). Atmospheric conditions were clear at the time of image acquisition, and the data had been corrected for the radiometric and geometric distortions of the images to the standard Level 1G before delivery.

2.4.2. Satellite image processing

All images pre-processing and processing was executed using the IDRISI GIS and Image Processing software (Eastman, 2006). Landsat 5 TM and MODIS were projected to the same Portuguese coordinate system (Hayford-Gauss, Datum Lisbon). Landsat 5 TM image geometric correction (Lillesand et al., 2004; Eastman, 2006) was made using ground control points (Toutin, 2004) and was radiometrically resampled by nearest neighbour. The overall root mean square (RMS) was 13.93 m. The TM raw digital numbers were then transformed to percent reflectance according Chavez (1996). MODIS data were brought to the same grid resolution as Landsat 5 TM (30 m) and it was coregistered to Landsat 5 TM image as base, with a RMS of 14.54 m. Supervised classifications of multispectral images were carried out, based in the Maximum Likelihood classifier (MLC) using the six reflective bands (1–5 and 7) of TM sensor, covering the spectral ranges from 0.45 to 1.75 μm and 2.09 to 2.35 μm. The cover types, pine and shrubs, were isolated and subsequently validated with the Corine Land Cover map from 2006 (CLC 06, IGP, 2010). These two maps were further used as mask and AGB estimations were made inside these areas.

2.4.3. Vegetation indices development

Vegetation indices, specially the Normalized Difference Vegetation Index (NDVI), have been extensively applied in studies of vegetation biomass (Atkinson et al., 2000; Chirici et al., 2007; Viana et al., 2009). The provided bands (1–5 and 7) from the TM sensor allowed to compute the Normalized Difference Vegetation Index (NDVI) as NDVI = (NIR − R)/(NIR + R), where Near-infrared (NIR) is radiation in waveband 4 and red (R) is radiation in waveband 3. NDVI measures both the amount of green vegetation and vegetation health, but it also is a basic indicator of changes in vegetation over space and time. The Global MOD13Q1 data includes the MODIS Normalized Difference Vegetation Index (NDVI) and a new Enhanced Vegetation Index (EVI) provided every 16 days at 250-m spatial resolution as a gridded level-3 product in the Sinusoidal projection (https://lpdaac.usgs.gov/lpdaac/products/modis_products_table/vegetation_indices/16_day_l3_global_250m/mod13q1). Additionally the Tasseled Cap transformation was performed, which is an orthogonal transformation, and the green vegetation index was expressed through the development of their second component (Eastman, 2006).

2.5. Direct Radiometric Relationships (DRR)

The field inventory data, within the GIS database, was superimposed on the TM and MODIS images data and then the individual pixel value (30 m × 30 m) and the nearest pixel values (90 m × 90 m) were attached to the field records. Regressions were performed for the two strata (pine forest and shrubs) individually and for all plots combined. The spectral information extracted from these images (NDVI, EVI and Tasseled Cap) was used as independent variables for developing regression models. Linear, logarithmic, exponential, power, and second-order polynomial functions were tested on the data. Multiple linear regressions were also tested to determine if a combination of several variables (e.g., crown closure, age, elevation, etc.) could improve the associations. The best models, for each stratum, were applied to the imagery data where the independent variable was derived, and the predicted aboveground biomass maps were produced. Depending on the applied model some biomass values predicted by the regression equations were negative. This happened in the low Vegetation index values, so these pixels were removed, because in reality negative biomass values are not possible. The imagery data in which the independent variable (vegetation index) presented the best regression with the AGB was subsequently used as predictor (auxiliary map) in the Regression-kriging spatial prediction method.

2.6. Geostatistical modelling

Geostatistics offers a collection of deterministic and statistical tools aimed at understanding and modelling spatial variability through prediction and simulation (Journel and Huijbregts, 1978; Goovaerts, 1997; Deutsch and Journel, 1998). Geostatistical procedures were performed with the GSTAT package included in IDRISI software both to automatically fit the variograms of residuals and to produce final predictions (Pebesma, 2001, 2004). GSTAT produces the predictions and variance map, which is the estimate of the uncertainty of the prediction model, i.e. precision of prediction. In this research, we employed Ordinary kriging (OK), Universal kriging (UK) and Regression-kriging (RK) spatial models. Geostatistical methods such as the semivariogram, also called the variogram, can be used to quantify the spatial variability of a random variable. The first stage of geostatistical modelling consists in computing the experimental variograms using the classical formula (Eq. (9)):

$$\hat{\gamma}(h) = \frac{1}{2N(h)} \sum_{i=1}^{N(h)} [z(x_i) - z(x_i + h)]^2 \quad (9)$$

where $\hat{\gamma}(h)$ is the semivariance for distance h, $N(h)$ the number of pairs for a certain distance and direction of h units, while $z(x_i)$ and $Z(x_i + h)$ are measurements at locations x_i and $x_i + h$, respectively.

Two variogram models were developed: one for the pine crown biomass and one for the shrub AGB, which is satisfactory according to Webster and Oliver (1992). For fitting the experimental variograms we used the exponential, Gaussian, spherical models using iterative reweighted least squares estimation (WLS, Cressie, 1993). Semivariogram gives a measure of spatial correlation of the studied attribute. The variogram is a discrete function of variogram values at all considered lags (Curran, 1988; Isaaks and Srivastava, 1989). Typically, the semivariance values exhibit an ascending behaviour near the origin of the variogram and they usually level off at larger distances (the sill of the variogram). The semivariance value at distances close to zero is called the nugget effect. The distance at which the semivariance levels off is the range of the variogram and represents the separation distance at which two samples can be considered to be spatially independent.

At locations where two properties u and v have been measured it is possible to estimate the cross-variogram. The cross-variogram is used to characterize spatial dependency between two variables. This is given as (Lloyd, 2007) (Eq. (10)):

$$\hat{\gamma}_{uv}(h) = \frac{1}{2N(h)} \sum_{i=1}^{N(h)} \{[z_u(x_i) - z_u(x_i + h)] \cdot [z_v(x_i) - z_v(x_i + h)]\} \quad (10)$$

where $\hat{\gamma}_{uv}(h)$ is the cross-semivariance between variables u and v, $N(h)$ is the number of pairs of data locations separated by lag distance h, z_u is the value of variable u at locations x_i and $(x_i + h)$ and z_v is the data value of variable v at the same locations.

2.7. Validation and assessment of the prediction techniques

To compare the different AGB prediction approaches, we examined the discrepancies between the known data and the predicted data. It is common to check the consistency of interpolation methods using the cross-validation procedure, in which each sample value is removed one at a time from the data set (Leave-One-Out), and that location is predicted from the remaining data (Goovaerts, 1997; Deutsch and Journel, 1998). However, according (Davis, 1987) cross-validation cannot confirm that a particular model is or is not the optimum. It is a method to better examine and understand the phenomenon under study using the available data. On other side, as we intended to compare the geostatistical approaches with the deterministic (IDW and Thiessen polygons) and DRR predictions, we adopted the methodology of dividing the locations randomly into two sets: the prediction set and the validation set. Webster and Oliver (1992) consider that more reliable estimation of semivariogram values requires at least 150 observations, and larger samples are needed to describe anisotropic direction-dependent variation. This does not mean, however, that geostatistics cannot be applied to smaller data sets (Goovaerts, 1997). The prediction approaches were evaluated by comparing the basic statistics of predicted AGB maps (i.e., mean and standard deviation) and the difference between the known data and the predicted data were examined using the mean error, or bias mean error (ME), the mean absolute error (MAE), standard deviation (SD) and the root mean squared error (RMSE), which measures the accuracy of predictions, as described in Eqs. (11)–(14).

$$SD = \sqrt{\frac{1}{N-1} \sum_{i=1}^{N} (e_i - \bar{e})^2} \quad (11)$$

Table 2
Allometric equations used to estimate biomass in the field plots.

Cover type	Equation	R^2
Pine	$AGB_{pine} = 19,284.26d^{2.299}h^{-07902}$	0.81
Shrub	$AGB_{Srb} = 0.0258[(Cc)(h_{srb})]^{0.754}$	0.89

Where AGB_{pine} is the crown biomass (kg tree^{-1}), d_{bh} is the diameter at breast height (m), h_t is the mean height of tree (m), h_c is the height of live canopy (m), AGB_{srb} is the biomass of srub (ton ha^{-1}), Cc is the crown closure (%) and h_{srb} is the mean height of shrubs (cm).

$$ME = \frac{1}{N} \sum_{i=1}^{N} (\hat{e}_i - e_i) \quad (12)$$

$$MAE = \frac{1}{N} \sum_{i=1}^{N} |\hat{e}_i - e_i| \quad (13)$$

$$RMSE = \sqrt{\frac{1}{N} \sum_{i=1}^{N} (\hat{e}_i - e_i)^2} \quad (14)$$

where N is the number of values in the dataset, $\hat{e}_i$ is the estimated biomass, e_i is the biomass values measured on the validation plots and $\bar{e}$ is the mean of biomass values of the sample.

3. Results and discussion

3.1. Descriptive statistics of study sites

The descriptive statistics of pine stands' crown biomass and shrubland's above-ground biomass, measured during field work and recorded in the inventory dataset, are presented in Table 1. The pine stands are highly heterogeneous, with ages ranging from 8 to 51 years old and the crown biomass ranging from 1.3 to 36 ton ha^{-1}. The shrubland areas are also heterogeneous, with canopy density ranging from 5 to 100%, and the biomass per hectare ranging from 0.79 to 36 ton ha^{-1}.

3.2. Above-ground biomass calculation from the inventory dataset

Based on the destructive sample approach, several allometric equations were adjusted, at plot level, to calculate the AGB in the inventory dataset. The analysis of the correlation coefficients (R), coefficients of determination (R^2), adjusted coefficients of determination (R^2_{adj}), the significance of the Student t-test, and the root mean square error (RMSE) allowed to select the best equations to predict the biomass of pine ($R^2 = 0.81$) and shrub ($R^2 = 0.89$), as presented in Table 2.

3.3. Relation between above-ground biomass and remote sensing data

The correlation analyses between calculated AGB in sample plots and predictors (spectral bands, vegetation indices, Tasseled Cap transformation, principal components), shows that vegetation indices were better correlated with biomass. Hence, several regression models were developed using stand-wise forest inventory data and Landsat TM and MODIS vegetation indices. The best results are presented in Table 3.

The best equations were achieved with NDVI derived from Landsat 5 TM, as independent variable, both for pine stands and shrub land, as presented in Fig. 2. The better results using the higher spatial resolution of Landsat TM data are due to the fact that the effect of mixed pixels is reduced compared to coarse resolution MODIS

Table 3
Regression models developed using stand-wise forest inventory data and Landsat 5 TM and MODIS image data.

Cover type	Model	Independent variable	α	β	δ	R^2	RMSE (ton ha^{-1})	Average predict biomass (ton ha^{-1})
Pine stands	$y=\alpha\cdot x^{\beta}$	NDVI (TM)	112.9820	2.4018		0.52	7.48	16.1
	$y=\alpha+\beta x+\delta x^2$		−14.0787	62.0106	25.335	0.49	7.24	17.7
	$y=\alpha\cdot e^{\beta x}$		1.0957	5.9478		0.51	7.88	16.2
	$y=\alpha+\beta x$		−18.4745	83.5498		0.49	7.22	17.7
	$y=\alpha\cdot x^{\beta}$	NDVI (MODIS)	49.2270	2.4034		0.22	6.52	15.1
	$y=\alpha+\beta x+\delta x^2$		−76.1399	271.2939	−188.857	0.17	9.28	17.7
	$y=\alpha\cdot e^{\beta x}$		1.2411	4.0514		0.21	9.89	15.1
	$y=\alpha+\beta x$		−12.1289	49.3060		0.15	9.35	17.7
	$y=\alpha\cdot x^{\beta}$	EVI (MODIS)	151.1559	2.0062		0.23	3.89	15.2
	$y=\alpha+\beta x+\delta x^2$		−34.9565	252.3460	−262.456	0.20	9.07	17.7
	$y=\alpha\cdot e^{\beta x}$		1.9357	6.3878		0.22	9.64	15.2
	$y=\alpha+\beta x$		−9.2017	85.6510		0.20	9.08	17.7
Shrubland	$y=\alpha\cdot x^{\beta}$	NDVI (TM)	33.9450	1.1064		0.50	5.73	10.5
	$y=\alpha+\beta x+\delta x^2$		2.9293	3.3927	57.4804	0.59	5.28	12.0
	$y=\alpha\cdot e^{\beta x}$		2.2121	4.1548		0.55	5.43	10.9
	$y=\alpha+\beta x$		−2.6106	42.6519		0.56	5.38	12.0
	$y=\alpha\cdot x^{\beta}$	NDVI (MODIS)	39.9192	2.2160		0.32	7.38	10.1
	$y=\alpha+\beta x+\delta x^2$		−12.5798	54.86892	−14.8373	0.25	7.12	12.0
	$y=\alpha\cdot e^{\beta x}$		0.9470	4.322952		0.31	7.45	10.1
	$y=\alpha+\beta x$		−8.6513	39.3024		0.25	7.08	12.0
	$y=\alpha\cdot x^{\beta}$	EVI (MODIS)	73.6125	1.5601		0.24	7.47	9.9
	$y=\alpha+\beta x+\delta x^2$		−4.7182	67.3874	−20.3535	0.23	7.19	12.0
	$y=\alpha\cdot e^{\beta x}$		2.1054	5.4164		0.23	7.51	9.9
	$y=\alpha+\beta x$		−3.0693	55.4241		0.23	7.16	12.0

Where y is the biomass (ton ha^{-1}) and α, β, δ are the coefficients of regression.

data. In TM data (30 m) the average reflectance of forest stands and shrubland is more pure than that of 250 m resolution MODIS pixels. These regression models were further used to map the biomass by the DRR method and the NDVI TM image was used as auxiliary variable in RK spatial prediction method.

3.4. Geostatistical predictions

To spatially estimate AGB by geostatistical modelling the experimental semivariograms were computed and analysed at first stage. The directional semivariograms of the residuals did not show an evident behaviour of anisotropy, thus an isotropic pattern was considered. The omnidirectional semivariograms were tested and its Exponential, Gaussian and Spherical models were fitted using Eq. (9). While the shrub biomass showed a clear spatial dependence (Fig. 3) the crown biomass of pine stands presented lower spatial autocorrelation (Fig. 4). The high nugget effect, visible in the figure, which under ideal circumstances should be zero, indicates that there is a significant amount of error present in the data due to the short scale variation, principally in pine data. In fact, in surveys covering large geographical regions, the residuals from the regression model may lack spatial structure because the large distances separating sample data locations. As reported by different authors (Gilbert and Lowell, 1997; Gunnarsson et al., 1998) forest variables are not always spatially continuous because it is highly dependent on forest landscape structure even to the densest sampling schema. In shrubland this is not so evident, since these areas have a higher spatial continuity, thus presenting an autocorrelation on the variable studied. For shrub, automated variograms modelling gave a small nugget and larger range parameter (6.35 km, 7.09 km and 13.09 km for exponential, Gaussian and spherical models, respectively), whereas for pine the range parameter was fairly shorter

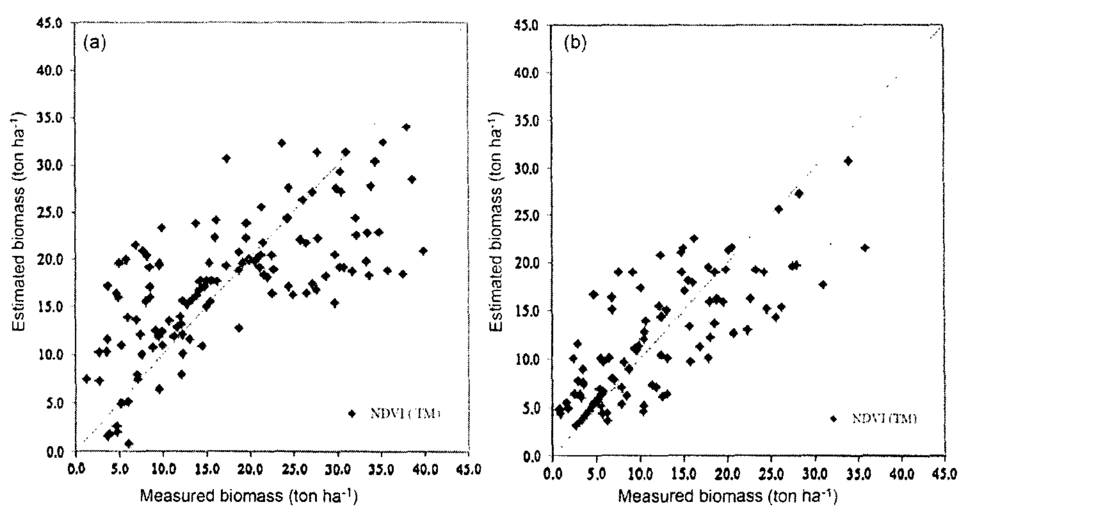

Fig. 2. Scatter plots of measured biomass versus estimated biomass from regression equations with NDVI as independent variable (a) pine and (b) shrubland. A 1:1 line (black, dashed) is provided for reference.

Table 4
Shrub and Pine AGB estimation models evaluation using the validation sample plots.

	ME (ton ha^{-1})		MAE (ton ha^{-1})		RMSE (ton ha^{-1})		SD (ton ha^{-1})	
	Pine	Shrub	Pine	Shrub	Pine	Shrub	Pine	Shrub
IDW	0.33	0.23	8.34	5.74	10.56	7.46	3.44	4.39
Thiessen	−0.39	8.89	9.10	10.30	11.68	12.23	10.34	6.20
DRR	0.62	0.34	3.93	2.87	5.60	3.69	7.84	4.85
OK (exponential)	1.35	0.52	6.77	6.18	8.02	7.60	4.24	4.39
OK (Gaussian)	1.46	0.77	6.76	6.41	7.79	7.52	4.03	4.01
OK (spherical)	1.36	0.65	6.80	6.36	8.03	7.56	4.17	4.07
UK (exponential)	1.17	0.39	6.59	6.35	7.64	7.57	3.09	4.69
UK (Gaussian)	1.37	0.22	6.87	6.25	8.06	7.62	4.11	4.82
UK (spherical)	1.32	0.48	6.60	5.69	7.71	6.85	3.61	3.47
RK (exponential)	0.61	0.74	4.05	3.65	5.46	4.33	8.11	5.82
RK (Gaussian)	0.55	1.01	4.09	3.99	5.52	4.61	8.16	5.98
RK (spherical)	0.62	0.75	4.04	3.65	5.53	4.27	8.13	5.77

(2.3 km, 2.9 km and 6.3 km for exponential, Gaussian and spherical models, respectively). Despite the exponential model fit better the shrub biomass (nugget of 22, a partial sill of 56, and a range of 6.35 km) and the spherical model fit better the pine stand biomass (nugget of 88, a partial sill of 19, and a range of 6.3 km) we used all the fitted models in the geostatistical spatial predictions (OK, UK and RK) to evaluate which is more effective in the predictions all over the study area.

3.5. *Validation of spatial distribution methods of above-ground biomass*

The validation of spatial prediction methods, based on random samples outside of the training data set, was made by comparing the basic statistics of predicted AGB maps (Table 4). In the pine AGB predictions 100 observations were used for the prediction and 32 for validation. In the shrub AGB predictions 81 observations were used for predictions and 21 for validation. Training and validation sets were compared, by means of a Student's *t* test (t_{pine} = 0.856 ns; t_{shrub} = 0.746 ns), in order to check if they provided unbiased subsets of the original data.

In both shrub and pine biomass estimations the mean error (ME), which should ideally be zero if the interpolation method is unbiased, suggests that all predictions are slightly biased. Analysing the mean absolute errors (MAE) it is clear that DRR approach achieved the lowest errors however, RK method had a similar performance. The archived RMSE in pine estimations was lower in RK than in DRR approach but in shrub estimations DRR provided inferior RMSE values than RK approach (Table 4 and Fig. 5). The best results in pine biomass predictions originated a RMSE = 32.2% of the mean (17.4 ton ha^{-1}) for DRR approach and a very similar result for the RK(exponential) approach, with a RMSE = 31.4% of the mean (17.4 ton ha^{-1}). Shrub biomass estimation based on DRR approach resulted in a RMSE = 31.8% of the mean (11.6 ton ha^{-1}) and RK(spherical) resulted in a RMSE = 35.6% of the mean (12 ton ha^{-1}).

Table 5
Results from ANOVA to compare the differences between the means of the different prediction methods.

Source	DF	SS	MS	*F*	*P*
Pine					
Between	11	279.5	25.407	0.65	0.7863
Within	372	14564.5	39.152		
Total	383	14844			
Shrub					
Between	11	1348.08	122.553	5.01	0
Within	240	5866.51	24.444		
Total	251	7214.59			

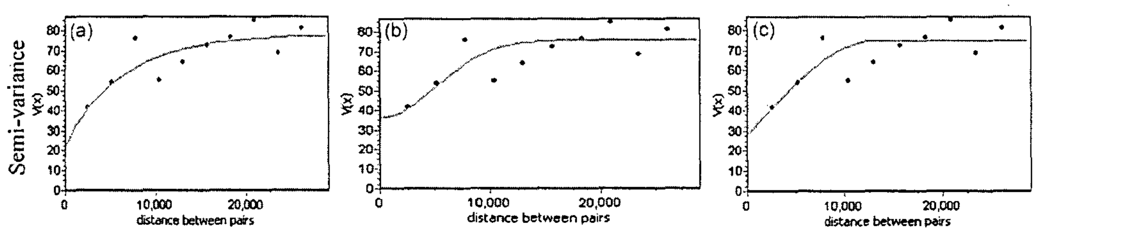

Fig. 3. Experimental omnidirectional semivariogram for shrub biomass: (a) exponential [22.000000 Nug(0) + 56 Exp(6350)]; (b) Gaussian [36.000000 Nug(0) + 40 Gau(7090)] and (c) spherical models [28.000000 Nug(0) + 47 Sph(13090)].

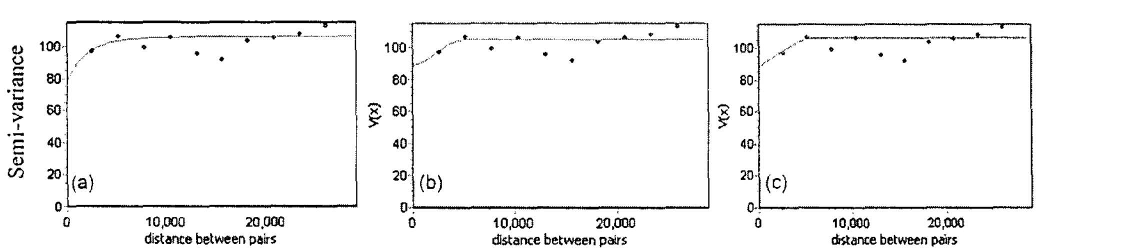

Fig. 4. Experimental omnidirectional semivariogram for pine biomass: (a) exponential [79.000000 Nug(0) + 28 Exp(2300)]; (b) Gaussian [89.000000 Nug(0) + 17 Gau(2900)] and (c) spherical models [88.000000 Nug(0) + 19 Sph(6300)].

Table 6
Tukey HSD all-pairwise comparisons test.

Method	Pine AGB		Shrub AGB	
	Mean	Tukey group	Mean	Tukey group
IDW	15.25	A	11.49	B
Thiessen	16.40	A	20.14	A
DRR	17.41	A	11.60	B
OK (exponential)	18.14	A	11.78	B
OK (Gaussian)	18.25	A	12.03	B
OK (spherical)	18.15	A	11.91	B
UK (exponential)	17.96	A	11.64	B
UK (Gaussian)	18.16	A	11.48	B
UK (spherical)	18.11	A	11.74	B
RK (exponential)	17.40	A	12.00	B
RK (Gaussian)	17.35	A	12.26	B
RK (spherical)	17.41	A	12.01	B

Table 7
Summary statistics of crown biomass of pine stands maps estimated from spatial prediction methods.

Method	Pixels	Area (ha)	Mean (ton ha^{-1})	Std (ton ha^{-1})	AGB (total ton)
IDW	842,408	75,816.7	18.24	5.70	1,383,156
Thiessen	842,408	75,816.7	18.08	10.31	1,370,511
DRR	815697	73,412.7	19.78	8.14	1,452,329
OK (exponential)	842,408	75,816.7	18.11	4.01	1,373,003
OK (Gaussian)	842,408	75,816.7	18.21	3.81	1,380,243
OK (spherical)	842,408	75,816.7	18.10	3.96	1,372,373
UK (exponential)	842,408	75,816.7	18.04	3.19	1,367,642
UK (Gaussian)	842,408	75,816.7	18.04	3.20	1,367,498
UK (spherical)	842,408	75,816.7	18.04	3.19	1,367,642
RK (exponential)	810,690	72,962.1	20.07	8.09	1,464,183
RK (Gaussian)	809,462	72,851.6	20.06	8.10	1,461,312
RK (spherical)	809,372	72,843.5	20.08	8.09	1,462,572

Table 8
Summary statistics of shrub AGB maps estimated from spatial prediction methods.

Method	Pixels	Area (ha)	Mean (ton ha^{-1})	Std (ton ha^{-1})	AGB (total ton)
IDW	1,268,228	114,141	11.36	4.46	1,296,347
Thiessen	1,268,228	114,141	10.83	8.13	1,235,867
DRR	1,268,228	114,141	10.80	5.54	1,232,276
OK (exponential)	1,268,228	114,141	11.69	4.02	1,333,860
OK (Gaussian)	1,268,228	114,141	11.85	3.88	1,352,688
OK (spherical)	1,268,228	114,141	11.83	3.85	1,350,573
UK (exponential)	1,268,228	114,141	11.67	4.62	1,331,610
UK (Gaussian)	1,268,228	114,141	11.62	4.63	1,326,543
UK (spherical)	1,268,228	114,141	11.90	3.45	1,357,917
RK (exponential)	1,237,251	111,353	11.18	5.98	1,245,362
RK (Gaussian)	1,238,493	111,464	11.22	6.01	1,250,744
RK (spherical)	1,238,644	111,478	11.23	6.00	1,251,459

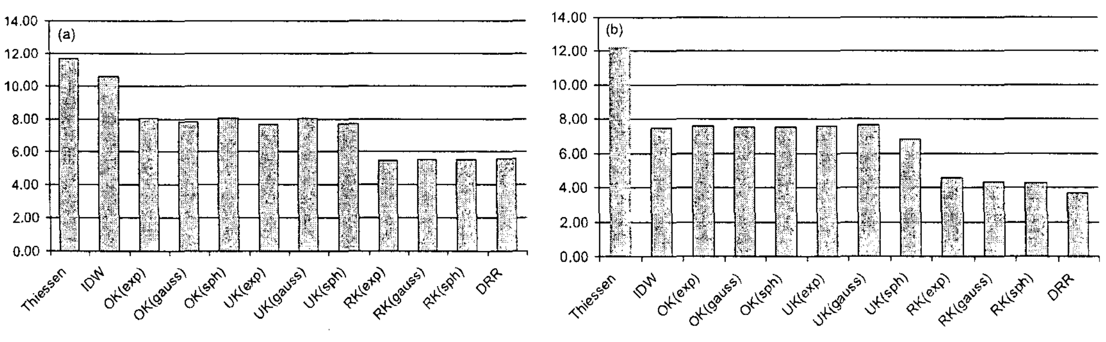

Fig. 5. Comparison of Root Mean Square Errors (RMSE) (a) pine and (b) shrub.

Table 9
Spatial correlation coefficients calculated between pine crown biomass maps.

	IDW	Thiessen	DRR	OK (exp)	OK (gauss)	OK (sph)	UK (exp)	UK (gauss)	UK (sph)	RK (exp)	RK (gauss)	RK (sph)
IDW	1											
Thiessen	0.81	1										
DRR	0.19	0.10	1									
OK (exponential)	0.74	0.49	0.26	1								
OK (Gaussian)	0.66	0.41	0.26	0.95	1							
OK (spherical)	0.70	0.46	0.27	1.00	0.95	1						
UK (exponential)	0.60	0.34	0.30	0.90	0.91	0.91	1					
UK (Gaussian)	0.60	0.34	0.30	0.90	0.91	0.91	1.00	1				
UK (spherical)	0.70	0.44	0.29	0.97	0.96	0.97	0.97	0.97	1			
RK (exponential)	0.28	0.17	0.99	0.35	0.34	0.35	0.37	0.37	0.37	1		
RK (Gaussian)	0.27	0.16	0.99	0.31	0.30	0.31	0.33	0.33	0.34	1.00	1	
RK (spherical)	0.25	0.15	0.99	0.30	0.29	0.30	0.33	0.33	0.33	1.00	1.00	1

Table 10
Spatial correlation coefficients calculated between shrub AGB map estimates.

	IDW	Thiessen	DRR	OK (exp)	OK (gauss)	OK (sph)	UK (exp)	UK (gauss)	UK (sph)	RK (exp)	RK (gauss)	RK (sph)
IDW	1											
Thiessen	0.84	1										
DRR	0.24	0.18	1									
OK (exponential)	0.90	0.73	0.28	1								
OK (Gaussian)	0.80	0.62	0.28	0.97	1							
OK (spherical)	0.84	0.66	0.29	0.98	0.99	1						
UK (exponential)	0.87	0.69	0.26	0.94	0.91	0.92	1					
UK (Gaussian)	0.87	0.72	0.26	0.94	0.92	0.93	0.99	1				
UK (spherical)	0.90	0.69	0.30	0.92	0.85	0.88	0.85	0.86	1			
RK (exponential)	0.42	0.35	0.90	0.44	0.42	0.42	0.41	0.41	0.40	1		
RK (Gaussian)	0.39	0.32	0.90	0.43	0.43	0.43	0.41	0.41	0.38	0.99	1	
RK (spherical)	0.41	0.35	0.90	0.42	0.41	0.41	0.40	0.40	0.39	1.00	0.99	1

The results indicate that determinists and geostatistical (OK and UK) approaches are not efficient to map these type of forest variables, as spatial structure in field biomass data is weak, as concluded by others (Gilbert and Lowell, 1997; Gunnarsson et al., 1998; Tuominen et al., 2003; Freeman and Moisen, 2007). Nevertheless, despite DRR was the most efficient method to map AGB, RK approach can be considered to explore in future studies with the aim of improve biomass estimation accuracy, were autocorrelation between variables exists.

In order to compare the mean values, of crown biomass and shrub biomass estimated by the interpolation methods, analysis of variance (ANOVA) was performed (Table 5). The results show that, at alpha level 0.05, the differences between the means are not significant between the pine AGB maps, but for shrub AGB maps the test failed to reject the null hypothesis that means were equal. Hence, the Tukey HSD All-Pairwise Comparisons Test was carried out to examine the differences between the interpolation methods used (Table 6). For pine AGB maps the test confirmed that there are no significant pairwise differences among the biomass means that emanated from all the interpolation methods used, but for shrub AGB maps there are 2 groups (A and B) in which the Thiessen method is statistically different from the other studied methods, as indicated in Table 6. Despite that, curiously, the average values of biomass were statistically similar between almost all methods, it just means that interpolations over large areas based on these methods (deterministic and geostatistical where there is no apparent autocorrelation of the variables) can be misleading. In fact, spatially explicit biomass estimation is only reliable by using remote sensing (e.g. DRR or k-NN) or by using remote sensing data, as auxiliary variable, in techniques such as RK, where the

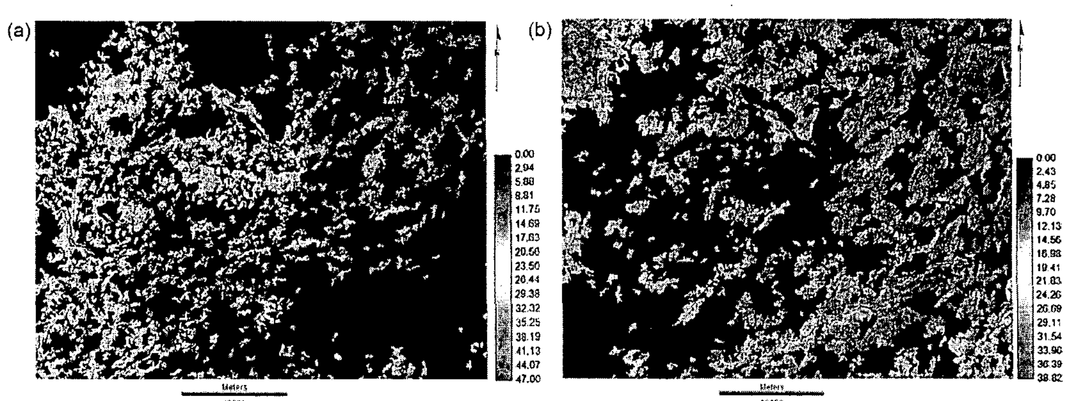

Fig. 6. Spatially explicit AGB estimates (ton ha^{-1}) for the study area (the colour gradation represents the vegetation and the black colour represents other land cover types, i.e. no data) generated from DRR spatial prediction method (a) pine stands and (b) shrubland.

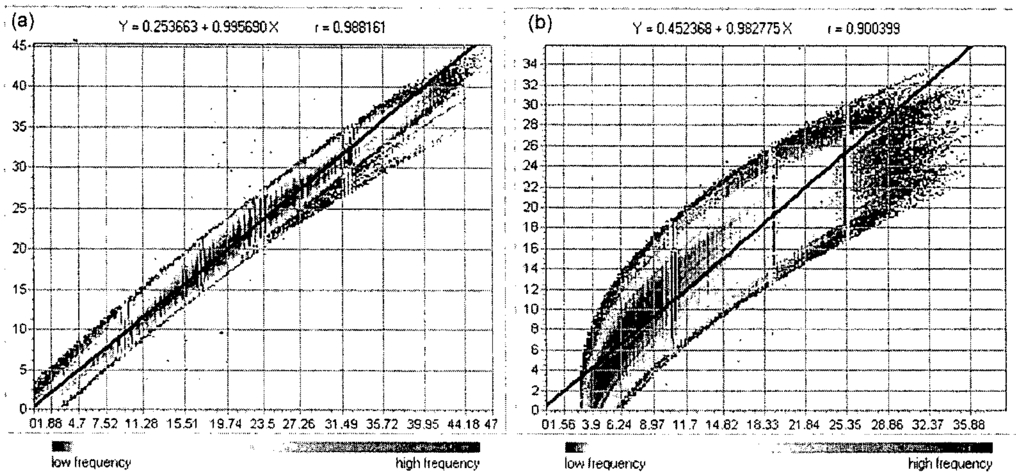

Fig. 7. Regression performed between DRR and RK Biomass maps, where x and y is the biomass in ton ha^{-1} (a) pine stands and (b) shrubland.

existence of autocorrelation between the variables could improve the estimates.

3.6. *Quantitative comparison of AGB mapping methods*

Estimates of the crown biomass of pine stands and shrubland AGB (ton ha^{-1}) are shown in Tables 7 and 8, respectively. Furthermore, Fig. 6 shows the biomass maps derived by DRR method for the entire study area. The biomass estimates, both the average values (ton ha^{-1}) and the total biomass, shows a clear distinction between the DRR and RK methods and the other spatial prediction methods. As concluded by the analysis of the statistics of the validation dataset, the deterministic approaches and Kriging methods are unsuitable to these mapping purposes as they tend to suppress variance of estimations (Tables 7 and 8). Hence, comparing the DRR and RK approaches the differences in the total biomass is less than 1% in the best estimates. Another interesting conclusion is that the differences between the total biomass estimated by RK approach are minor using the Exponential, Gaussian or Spherical models in the experimental variogram. The correlation coefficients, presented in Tables 9 and 10 calculated for comparing pine and shrub AGB maps, respectively, confirm the similar results between DRR and RK estimations. Fig. 7a and b shows the high correlation existent between the two biomass maps (DRR × RK) of pine stand and shrubland, respectively.

Despite these results, RK method did not improve the biomass map estimation, given the low spatial autocorrelation observed on the data (Figs. 3 and 4). However, this method can be exploited in the case of geographical location of sample plots are denser, or forested areas have a greater spatial continuity, not being so dependent on forest landscape structure and boundary lines of forest patches, as these Mediterranean forests.

4. Conclusion

This study compared the spatial prediction methods Direct Radiometric Relationships (DRR) and Regression-kriging (RK), to estimate crown biomass of *P. pinaster* stands and shrubland above-ground biomass. Moreover, Ordinary Kriging (OK), Universal Kriging (UK), Inverse Distance Weighted (IDW) and Thiessen Polygons estimations were performed. The results showed, as expected, that the deterministic approaches are not suitable for mapping biomass. The same occurs with geostatistical interpolation methods as kriging, as they are dealing with the idea that it occurs spatial autocorrelation between neighbouring field measurement points, which is not a reality in the scattered mosaic of the studied forest landscape. However, as in much of the time the users employ spatial prediction techniques to visually understand the distribution of biomass, Kriging or deterministic models can be used, as they are easily implemented. Remote sensing is the only way, to provide spatially distributed information of the landscape structure (Jong et al., 2006) of intermediate areas between field measurements so, methods using remotely sensed data, as DRR, are the suitable way to map biomass. RK predictions, using remotely sensed data as auxiliary predictor, did not improve the AGB estimations, which is associated to the low spatial dependence observed on the data. Thus, denser sampling schemes and different auxiliary variables should be explored, in order to test if the accuracy of predictions is improved.

The results provided by DRR and RK methods showed the advantages of using the association between remotely sensed data and ground inventory data in spatial mapping. However, it should be noted that the cover types under study presented a homogeneous diversity (pure pine stands and shrubland) which allows a moderately to high correlation between vegetation characteristics and spectral response. Thus, if the objective is to map heterogeneous land cover types (e.g. mixed stands, different crown closure, etc.) the differences between spectral characteristics will increase, which will add noise to the prediction models based in remote sensed data. So, stratification of forest cover should be needed before using this approach.

The RK method has the advantage of generating estimates for the spatial distribution of AGB and its uncertainty for the study area. The uncertainty maps allow the evaluation of the reliability of estimates by identifying the locals with major uncertainties which can be useful for example to select different estimation methods for those areas.

Despite RK has been increasingly used, this method has some obstacles which difficult its popularization. Since then, different names and approaches are presented in the literature about the regression-kriging theory, which leads to a confusion by the common users. An additional limitation is that RK is more sophisticated and computationally demanding than other techniques, and therefore still exist a lack of user-friendly GIS environments to run RK.

Independently of the spatial prediction method applied, these techniques are a complement to the traditional field inventories as surveys continue to be needed to collect the input data and to assess the results of spatial prediction.

Acknowledgement

Authors would like to express their acknowledgement to the Portuguese Science and Technology Foundation (FCT), programme SFRH/PROTEC/49626/2009.

References

Ahmed, S., De Marsily, G., 1987. Comparison of geostatistical methods for estimating transmissivity using data on transmissivity and specific capacity. Water Resources Research 23, 1717–1737.

Akhavan, R., Kia-Daliri, H., 2010. Spatial variability and estimation of tree attributes in a plantation forest in the Caspian region of Iran using geostatistical analysis Caspian. Journal of Environmental Sciences 8, 163–172.

Atkinson, P.M., Foody, G.M., Curran, P.J., Boyd, D.S., 2000. Assessing the ground data requirements for regional scale remote sensing of tropical forest biophysical properties. International Journal of Remote Sensing 21, 2571–2587.

Atkinson, P.M., Tatnall, A.R.L., 1997. Introduction neural networks in remote sensing. International Journal of Remote Sensing 18, 699–709.

Berterretche, M., Hudak, A.T., Cohen, W.B., Maiersperger, T.K., Gower, S.T., Dungan, J., 2005. Comparison of regression and geostatistical methods for mapping Leaf Area Index (LAI) with Landsat ETM+ data over a boreal forest. Remote Sensing of Environment 96, 49–61.

Blackard, J.A., Dean, D.J., 1999. Comparative accuracies of artificial neural networks and discriminant analysis in predicting forest cover types from cartographic variables. Computers and Electronics in Agriculture 24, 131–151.

Brown, S., Gillespie, A.J.R., Lugo, A.E., 1989. Biomass estimation methods for tropical forests with applications to forest inventory data. Forest Science 35, 881–902.

Brown, S., Lugo, A., 1992. Aboveground biomass estimates for tropical moist forests of Brazilian Amazon. Interciencia 17, 8–18.

Buddenbaum, H., Schlerf, M., Hill, J., 2005. Classification of coniferous tree species and age classes using hyperspectral data and geostatistical methods. International Journal of Remote Sensing 26, 5453–5465.

Burrough, P.A., McDonnell, R.A., 1998. Principles of Geographical Information Systems. Oxford University Press Inc., New York, 333 pp.

Chavez, P.S.J., 1996. Image-based atmospheric corrections-revisited and improved. Photogrammetric Engineering and Remote Sensing 62, 1025–1036.

Chirici, G., Barbati, A., Corona, P., Marchetti, M., Travaglini, D., Maselli, F., Bertini, R., 2008. Non-parametric and parametric methods using satellite images for estimating growing stock volume in alpine and Mediterranean forest ecosystems. Remote Sensing of Environment 112, 2686–2700.

Chirici, G., Barbati, A., Maselli, F., 2007. Modelling of Italian forest net primary productivity by the integration of remotely sensed and GIS data. Forest Ecology and Management 246, 285–295.

Cohen, W.B., Maiersperger, T.K., Gower, S.T., Turner, D.P., 2003. An improved strategy for regression of biophysical variables and Landsat ETM+ data. Remote Sensing of Environment 84, 561–571.

Cohen, W.B., Maiersperger, T.K., Spies, T.A., Oetter, D.R., 2001. Modelling forest cover attributes as continuous variables in a regional context with Thematic Mapper data. International Journal of Remote Sensing 22, 2279–2310.

Cressie, N.A.C., 1993. Statistics for Spatial Data. John Wiley & Sons, New York, USA, 416 pp.

Curran, P.J., 1988. The semivariogram in remote sensing: an introduction. Remote Sensing of Environment 24, 493–507.

Curran, P.J., Atkinson, P.M., 1988. Geostatistics and remote sensing. Progress in Physical Geography 22, 61–78.

Davis, B., 1987. Uses and abuses of cross-validation in geostatistics. Mathematical Geology 19, 241–248.

Deutsch, C.V., Journel, A.G., 1998. Geostatistical Software Library and User's Guide, 2nd ed. Oxford University Press, New York, USA, 369 pp.

Dungan, J., 1998. Spatial prediction of vegetation quantities using ground and image data. International Journal of Remote Sensing 19, 267–285.

Eastman, J.R., 2006. Idrisi Andes. Guide to GIS and Image Processing. Clark Labs, Clark University, USA, 328 pp.

Fearnside, P.M., 1992. Forest biomass in Brazilian Amazônia: comments on the estimate by Brown and Lugo. Interciencia 17, 19–27.

Fearnside, P.M., 1997. Greenhouse gases from deforestation in Brazilian Amazonia: net committed emissions. Climatic Change 35, 321–360.

Foroughbakhch, R., Reyes, G., Alvarado-Vázquez, M.A., Hernández-Piñero, J., Rocha-Estrada, A., 2005. Use of quantitative methods to determine leaf biomass on 15 woody shrub species in northeastern Mexico. Forest Ecology and Management 216, 359–366.

Fournier, R.A., Luther, J.E., Guindon, L., Lambert, M.C., Piercey, D., Hall, R.J., Wulder, M.A., 2003. Mapping aboveground tree biomass at the stand level from inventory information: test cases in Newfoundland and Quebec. Canadian Journal of Forest Research 33, 1846–1863.

Freeman, E., Moisen, G., 2007. Evaluating kriging as a tool to improve moderate resolution maps of forest biomass. Environmental Monitoring and Assessment 128, 395–410.

García-Martín, A., Pérez-Cabello, F., de la Riva, J.R., Montorio, R., 2008. Estimation of crown biomass of Pinus spp. from Landsat TM and its effect on burn severity in a Spanish fire scar. IEEE Journal of Selected Topics in Applied Earth Observations and Remote Sensing 1, 254–265.

Gilbert, B., Lowell, K., 1997. Forest attributes and spatial autocorrelation and interpolation: effects of alternative sampling schemata in the boreal forest. Landscape and Urban Planning 37, 235–244.

Gillespie, A.J.R., Brown, S., Lugo, A.E., 1992. Tropical forest biomass estimation from truncated stand tables. Forest Ecology and Management 48, 69–87.

Goovaerts, P., 1997. Geostatistics for Natural Resources Evaluation. Oxford University Press, Inc., New York, USA.

Goovaerts, P., 1999. Using elevation to aid the geostatistical mapping of rainfall erosivity. Catena 34 (3-4), 227–242.

Gunnarsson, F., Holm, S., Holmgren, P., Thuresson, T., 1998. On the potential of Kriging for forest management planning. Scandinavian Journal of Forest Research 13, 237–245.

Hame, T., Salli, A., Andersson, K., Lohi, A., 1997. A new methodology for the estimation of biomass of conifer dominated boreal forest using NOAA AVHRR data. International Journal of Remote Sensing 18, 3211–3243.

Hengl, T., 2009. A Practical Guide to Geostatistical Mapping, 2nd ed. University of Amsterdam, Amsterdam.

Hengl, T., Heuvelink, G.B.M., Rossiter, D.G., 2007. About regression-kriging: from equations to case studies. Computers & Geosciences 33, 1301–1315.

Hengl, T., Heuvelink, G.B.M., Stein, A., 2004. A generic framework for spatial prediction of soil variables based on regression-kriging. Geoderma 120, 75–93.

Hernández, J., Emery, X., 2009. A geostatistical approach to optimize sampling designs for local forest inventories. Canadian Journal of Forest Research 39, 1465–1474.

Hese, S., Lucht, W., Schmullius, C., Barnsley, M., Dubayah, R., Knorr, D., Neumann, K., Riedel, T., Schröter, K., 2005. Global biomass mapping for an improved understanding of the CO_2 balance—the Earth observation mission Carbon-3D. Remote Sensing of Environment 94, 94–104.

Houghton, R.A., Lawrence, K.T., Hackler, J.L., Brown, S., 2001. The spatial distribution of forest biomass in the Brazilian Amazon: a comparison of estimates. Global Change Biology 7, 731–746.

Hu, H., Wang, G.G., 2008. Changes in forest biomass carbon storage in the South Carolina Piedmont between 1936 and 2005. Forest Ecology and Management 255, 1400–1408.

IGP, 2010. CLC2006 – Cartografia CORINE Land Cover 2006 Para Portugal Continental; 2009 (verified 01.01.2010) http://www.igeo.pt/gdr/projectos/clc2006/.

Isaaks, E.H., Srivastava, R.M., 1989. An Introduction to Applied Geostatistics. Oxford University Press, New York, USA, 542 pp.

Iverson, L.R., Brown, S., Prasad, A., Mitasova, H., Gillespie, A.J.R., Lugo, A.E., 1994. Use of GIS for estimating potential and actual forest biomass for continental South and Southeast Asia. In: Dale, V.H. (Ed.), Effects of Land-Use Change on Atmospheric CO_2 Concentrations: South and Southeast Asia as a Case Study. Springer-Verlag, New York, pp. 67–116.

Jong, S.M.d., Pebesma, E.J., Meer, F.D.v.d., 2006. Spatial variability, mapping methods, image analysis and pixels. In: Jong, S.M.d., Meer, F.D.v.d. (Eds.), Remote Sensing Image Analysis: Including the Spatial Domain, vol. 5. Springer, Netherlands, pp. 17–35.

Journel, A.G., Huijbregts, C.J., 1978. Mining Geostatistics. Academic Press, London.

Kint, V., van Meirvenne, M., Nachtergale, L., Geudens, G., Lust, N., 2003. Spatial methods for quantifying forest stand structure development: a comparison between nearest-neighbor indices and variogram analysis. Forest Science 49, 36–49.

Knotters, M., Brus, D.J., Oude Voshaar, J.H., 1995. A comparison of kriging, co-kriging and kriging combined with regression for spatial interpolation of horizon depth with censored observations. Geoderma 67, 227–246.

Krige, D.G., 1951. A Statistical Approach to some Mine Valuations and Allied Problems at the Witwatersrand. University of Witwatersrand, South Africa.

Labrecque, S., Fournier, R.A., Luther, J.E., Piercey, D., 2006. A comparison of four methods to map biomass from Landsat-TM and inventory data in western Newfoundland. Forest Ecology and Management 226, 129–144.

Lillesand, T.M., Kiefer, R.W., Chipman, J.W., 2004. Remote Sensing and Image Interpretation, 5th ed. John Wiley and Sons Inc., New York, 764 pp.

Lloyd, C.D., 2007. Local Models for Spatial Analysis. CRC Press, Taylor & Francis Group, Boca Raton, pp. 244.

Lu, D., 2006. The potential and challenge of remote sensing based biomass estimation. International Journal of Remote Sensing 27, 1297–1328.

Lu, G.Y., Wong, D.W., 2008. An adaptive inverse-distance weighting spatial interpolation technique. Computers & Geosciences 34, 1044–1055.

Magcale-Macandog, D.B., Delgado, M.E.M., Ty, E., Villarin, J.R.T.A., 2006. A Gis-based model to improve estimation of aboveground biomass of secondary forests in the Philippines. Journal of Tropical Forest Science 18, 8–21.

Mandallaz, D., 1993. Geostatistical Methods for Double Sampling Schemes: Application to Combined Forest Inventories. Chair of Forest Inventory and Planning, Swiss Federal Institute of Technology (ETH), Zürich, p. 133.

Maselli, F., Chiesi, M., 2006. Evaluation of Statistical Methods to Estimate Forest Volume in a Mediterranean Region. IEEE Transactions on Geoscience and Remote Sensing 44, 2239–2250.

Matheron, G., 1963. Principles of geostatistics. Economic Geology 58, 1246–1266.

Matheron, G., 1969. Le krigeage Universel, vol. 1. Cahiers du Centre de Morphologie Mathematique, Ecole des Mines de Paris, Fontainebleau, 83 pp.

Matheron, G., 1971. The Theory of Regionalised Variables and its Applications. Les Cahiers du Centre de Morphologie Mathematique de Fontainblue, Ecole Nationale Superiore de Paris, Paris, 212 pp.

McBratney, A.B., Webster, R., 1981. The design of optimal sampling schemes for local estimation and mapping of regionalized variables—II: program and examples. Computers & Geosciences 7, 335–365.

McRoberts, R.E., Tomppo, E.O., Næsset, E., 2010. Advances and emerging issues in national forest inventories. Scandinavian Journal of Forest Research 25, 368–381.
Meng, Q., Cieszewski, C., Madden, M., 2009. Large area forest inventory using Landsat ETM+: a geostatistical approach. ISPRS Journal of Photogrammetry and Remote Sensing 64, 27–36.
Mutanga, O., Rugege, D., 2006. Integrating remote sensing and spatial statistics to model herbaceous biomass distribution in a tropical savanna. International Journal of Remote Sensing 27, 3499–3514.
Muukkonen, P., Heiskanen, J., 2005. Estimating biomass for boreal forests using ASTER satellite data combined with standwise forest inventory data. Remote Sensing of Environment 99, 434–447.
Muukkonen, P., Heiskanen, J., 2007. Biomass estimation over a large area based on standwise forest inventory data and ASTER and MODIS satellite data: a possibility to verify carbon inventories. Remote Sensing of Environment 107, 617–624.
Nanos, N., Calama, R., Montero, G., Gil, L., 2004. Geostatistical prediction of height/diameter models. Forest Ecology and Management 195, 221–235.
Odeh, I.O.A., McBratney, A.B., Chittleborough, D.J., 1994. Spatial prediction of soil properties from landform attributes derived from a digital elevation model. Geoderma 63, 197–214.
Odeh, I.O.A., McBratney, A.B., Chittleborough, D.J., 1995. Further results on prediction of soil properties from terrain attributes: heterotopic cokriging and regression-kriging. Geoderma 67, 215–226.
Palmer, D.J., Höck, B.K., Kimberley, M.O., Watt, M.S., Lowe, D.J., Payn, T.W., 2009. Comparison of spatial prediction techniques for developing Pinus radiata productivity surfaces across New Zealand. Forest Ecology and Management 258, 2046–2055.
Pebesma, E.J., 2001. Gstat User's Manual. University of Utrecht, 108 pp.
Pebesma, E.J., 2004. Multivariable geostatistics in S: the gstat package. Computers & Geosciences 30, 683–691.
Peichl, M., Arain, M.A., 2007. Allometry and partitioning of above- and belowground tree biomass in an age-sequence of white pine forests. Forest Ecology and Management 253, 68–80.
Pierce, K.B., Ohmann, J.L., Wimberly, M.C., Gregory, M.J., Fried, J.S., 2009. Mapping wildland fuels and forest structure for land management: a comparison of nearest neighbor imputation and other methods. Canadian Journal of Forest Research 39, 1901–1916.
Reese, H., Nilsson, M., Sandström, P., Olsson, H., 2002. Applications using estimates of forest parameters derived from satellite and forest inventory data. Computers and Electronics in Agriculture 37, 37–55.
Reich, R.M., Aguirre-Bravo, C., Bravo, V.A., Briseño, M.M., 2011. Empirical evaluation of confidence and prediction intervals for spatial models of forest structure in Jalisco, Mexico. Journal of Forestry Research 22, 159–166.
Reich, R.M., Lundquist, J.E., Bravo, V.A., 2004. Spatial models for estimating fuel loads in the Black Hills, South Dakota. International Journal of Wildland Fire 13, 119–129.
Sales, M.H., Souza Jr., C.M., Kyriakidis, P.C., Roberts, D.A., Vidal, E., 2007. Improving spatial distribution estimation of forest biomass with geostatistics: a case study for Rondônia, Brazil. Ecological Modelling 205, 221–230.
Sen, Z., 2009. Spatial Modeling Principles in Earth Sciences. Springer, Dordrecht/Heidelberg/London/New York, 351 pp.
Ter-Mikaelian, M.T., Korzukhin, M.D., 1997. Biomass equations for sixty-five North American tree species. Forest Ecology and Management 97, 1–24.
Tomppo, E., 1991. Satellite image-based national forest inventory of Finland. In: Proceedings of the Symposium on Global and Environmental Monitoring, Techniques and Impacts, International Archives of Photogrammetry and Remote Sensing, Victoria, British Columbia, Canada, pp. 419–424.
Tomppo, E., Nilsson, M., Rosengren, M., Aalto, P., Kennedy, P., 2002. Simultaneous use of Landsat-TM and IRS-1C WiFS data in estimating large area tree stem volume and aboveground biomass. Remote Sensing of Environment 82, 156–171.
Tomppo, E., Olsson, H., Ståhl, G., Nilsson, M., Hagner, O., Katila, M., 2008. Combining national forest inventory field plots and remote sensing data for forest databases. Remote Sensing of Environment 112, 1982–1999.
Toutin, T., 2004. Review article: geometric processing of remote sensing images: models, algorithms and methods. International Journal of Remote Sensing 25, 1893–1924.
Tuominen, S., Fish, S., Poso, S., 2003. Combining remote sensing, data from earlier inventories, and geostatistical interpolation in multisource forest inventory. Canadian Journal of Forest Research 33, 624–634.
Viana, H., Cohen, W.B., Lopes, D., Aranha, J., 2010. Assessment of forest biomass for use as energy. GIS-based analysis of geographical availability and locations of wood-fired power plants in Portugal. Applied Energy 87, 2551–2560.
Viana, H., Lopes, D., Aranha, J., 2009. Predição de biomassa arbustiva lenhosa empregando dados de inventário e o índice de diferença normalizada extraído em imagens landsat 5 TM. ISPV Millenium.
Weber, D., Englund, E., 1992. Evaluation and comparison of spatial interpolators. Mathematical Geology 24, 381–391.
Webster, R., Oliver, M.A., 1992. Sample adequately to estimate variograms of soil properties. Journal of Soil Science 43, 177–192.
Webster, R., Oliver, M.A., 2007. Geostatistics for Environmental Scientists, 2nd ed. John Wiley & Sons Ltd, England, 332 pp.
Woodcock, C.E., Strahler, A.H., Jupp, D.L.B., 1988. The use of variograms in remote sensing: II. Real digital images. Remote Sensing of Environment 25, 349–379.
Zhang, C., Franklin, S.E., 2002. Forest structure classification using airborne multispectral image texture and kriging analysis. In: IEEE International Geoscience and Remote Sensing Symposium, 2002. IGARSS '02, p. 2002.
Zheng, D., Heath, L.S., Ducey, M.J., 2007. Forest biomass estimated from MODIS and FIA data in the Lake States: MN, WI and MI, USA. Forestry 80, 265–278.
Zianis, D., Muukkonen, P., Mäkipää, R., Mencuccini, M., 2005. Biomass and Stem Volume Equations for Tree Species in Europe, Silva Fennica Monographs 4. Finnish Society of Forest Science, pp. 63.